

Journal of Biomedical Optics

SPIEDigitalLibrary.org/jbo

Optical properties of human skin

Tom Lister
Philip A. Wright
Paul H. Chappell



Optical properties of human skin

Tom Lister,^{a,b} Philip A. Wright,^a and Paul H. Chappell^b

^aWessex Specialist Laser Centre, Salisbury District Hospital, Salisbury, SP2 8BJ, United Kingdom

^bUniversity of Southampton, School of Electronics and Computer Science, Southampton, SO17 1BJ, United Kingdom

Abstract. A survey of the literature is presented that provides an analysis of the optical properties of human skin, with particular regard to their applications in medicine. Included is a description of the primary interactions of light with skin and how these are commonly estimated using radiative transfer theory (RTT). This is followed by analysis of measured RTT coefficients available in the literature. Orders of magnitude differences are found within published absorption and reduced-scattering coefficients. Causes for these discrepancies are discussed in detail, including contrasts between data acquired *in vitro* and *in vivo*. An analysis of the phase functions applied in skin optics, along with the remaining optical coefficients (anisotropy factors and refractive indices) is also included. The survey concludes that further work in the field is necessary to establish a definitive range of realistic coefficients for clinically normal skin. © 2012 Society of Photo-Optical Instrumentation Engineers (SPIE). [DOI: 10.1117/1.JBO.17.9.090901]

Keywords: skin optics; radiative transfer theory; absorption; scatter; melanin; hemoglobin.

Paper 12354V received Jun. 6, 2012; revised manuscript received Jul. 31, 2012; accepted for publication Jul. 31, 2012; published online Sep. 24, 2012.

1 Introduction

The color of human skin has long been used as a subjective adjunct to the detection and diagnosis of disease. More recently, the introduction of skin color measurements has extended this to include the potential for objective determination of skin features,¹ including melanin and hemoglobin concentrations,^{2–6} the depth and diameter of blood vessels,^{7–9} the depth of pigmented skin lesions,^{10,11} the maturity and depth of bruises,^{12,13} and keratin fiber arrangements.¹⁴

Such advances have proved invaluable for the advancement of skin laser treatments¹⁵ and photodynamic therapy,^{16–18} and have contributed to further advances in the diagnosis of cancerous and noncancerous skin lesions.^{10,19–21}

However, the success of these methods depends entirely upon adequate knowledge of the behavior of light as it impinges upon, and travels through, the skin. This article presents a description of the major interactions of visible light with skin and the principal skin features that contribute to these. This is followed by an analysis of published optical coefficients used in simulations of light transport through skin.

2 Background

2.1 Absorption

Absorption describes a reduction in light energy. Within the visible region, there are two substances generally considered to dominate the absorption of light in skin: hemoglobin and melanin.

Hemoglobin is the dominant absorber of light in the dermis. Normal adult hemoglobin (Hb A) is a protein consisting four polypeptide chains, each of which is bound to a heme.²² The heme in Hb A is named iron-photoporphyrin IX^{23,24} and is responsible for the majority of light absorption in blood. The free-electron molecular-orbital model describes this absorption

as an excitation of loosely bound “unsaturation electrons” or “ π -electrons” of the heme.²⁵ Within the visible region, Hb A contains three distinctive peaks. The dominant peak is in the blue region of the spectrum and is referred to as the Soret peak or Soret band. Two further peaks can be distinguished in the green-yellow region, between 500 and 600 nm, that in combination with the Soret band cause Hb A to appear red. These are known as the α and β bands, or collectively as the Q -band, and have intensities of around 1% to 2% of the Soret band.²⁶ The excitation levels of π -electrons vary, and therefore the positions and intensities of these bands vary with the ligand state of the heme (Fig. 1).

Melanins are ordinarily contained within the epidermis and produce an absorption spectrum that gradually decreases from the ultraviolet (UV) to the infrared (IR) regions. In contrast to hemoglobin, the variation and complexity of melanins means that their detailed structures are not yet fully understood, despite intense research over the last five decades, and this broadband absorbance spectrum is still a topic of scientific debate.^{5,28,29} At present, the scientific consensus appears to gravitate towards a chemical disorder model.^{5,28–33} This model proposes that melanins consist of a collection of oligomers or polymers in various forms arranged in a disordered manner. This results in a number of absorption peaks that combine to create a broadband absorbance effect^{28,30} (Fig. 2).

Further absorption of light may be attributed to chromophores, such as bilirubin and carotene,³⁴ lipids,³⁵ and other structures, including cell nuclei and filamentous proteins.^{36,37} Although the individual contributions from these secondary chromophores may be considered separately,^{13,38,39} most simulations group them into a single overarching value.^{40,41}

Despite its abundance in all tissues, water is not a significant absorber of light in the visible region, although its contribution has been considered when simulating skin color.⁴²

Address all correspondence to: Tom Lister, Wessex Specialist Laser Centre, Salisbury District Hospital, Salisbury, SP2 8BJ, United Kingdom. Tel: 01722780104; E-mail: tom.lister@soton.ac.uk

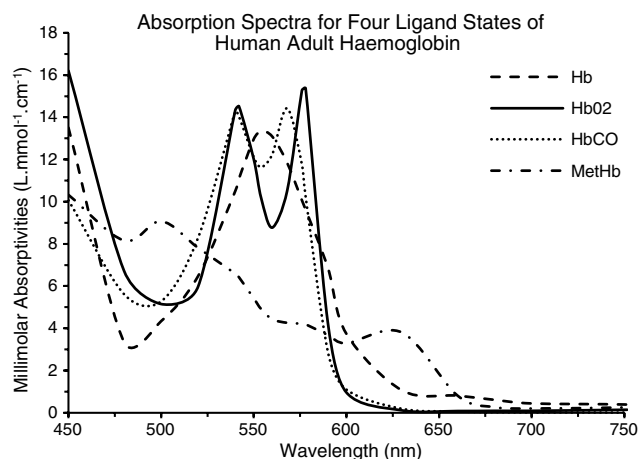


Fig. 1 Absorption spectra of deoxyhemoglobin (Hb), oxyhemoglobin (HbO₂), carboxyhemoglobin (HbCO), and methemoglobin (MetHb) in the visible region, from Ref. 27.

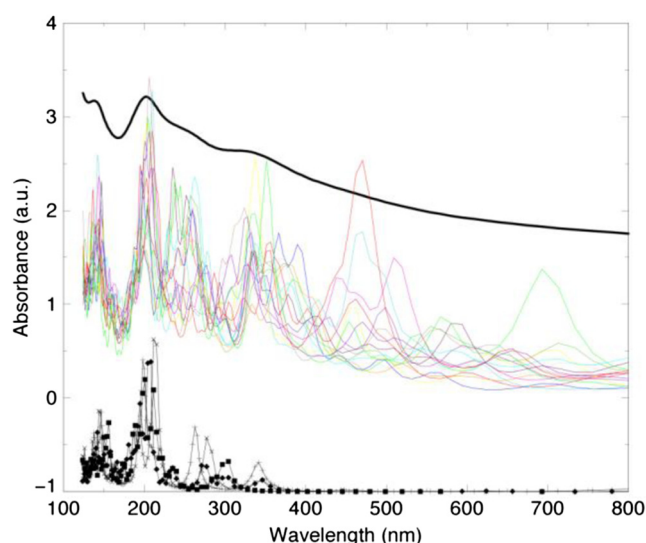


Fig. 2 Colored lines show individual absorption spectra of tetramer subunits within melanin extracted from human epidermis. The average absorption spectrum of these is shown by thick black line, shifted up 1.5 units for clarity. Thin black lines shifted down by one unit represent absorption spectra from monomer subunits. a.u. = arbitrary units. Reprinted figure with permission from Ref. 30.

2.2 Scattering

As well as absorption, scattering contributes significantly to the appearance of skin. Scattering describes a change in the direction, polarization or phase of light and is commonly portrayed as either a surface effect (such as reflection or refraction) or as an interaction with a small region whose optical properties differ from its surroundings (particulate scatter).

It has been estimated that 4% to 7% of visible light is reflected from the surface of the skin, independent of wavelength and skin color.^{43,44} The remaining light is refracted as it passes from air into the skin.

The primary sources of particulate scatter within the skin are filamentous proteins. Keratins are the filamentous proteins of the epidermis and form this layer's major constituent, whereas

collagen is the principal filamentous protein of the dermis and occupies approximately 18% to 30% of its volume.⁴⁵ Further scatter is attributed to melanosomes in the epidermis, cell nuclei, cell walls and many other structures in the skin that occur in smaller numbers.⁴⁶

Scatter from filamentous proteins has been approximated using a Mie solution to Maxwell's equations applied to data from *in vitro* skin samples.^{47,48} This approach provides an increase in simulated scattering probability with increasing fiber diameter and decreasing wavelength. The dependence of scatter on fiber diameter suggests that the protein structures of the dermis, which may be 10 times as large as those in the epidermis,^{45,49} possess a greater scattering cross-section. This in part compensates for the lower number densities of filamentous proteins in the dermis. The scattering events that occur are mainly in the forward direction, meaning that on average, light that returns to the surface undergoes a large number of scattering events.⁵⁰ One implication of the wavelength dependence of scatter is that blue and green light that has returned to the surface of the skin will have, on average, travelled less deeply than red light. This is considered the primary reason why blood vessels and pigmented nevi that are situated deeper within the skin are only able to absorb light from the red end of the spectrum and therefore appear bluer than their superficial equivalents.^{51,52}

The volume fraction of melanosomes in the epidermis varies typically from 1% in pale skin to 5% in darker skin,⁵³ although one group has suggested greater values.^{54,55} However, despite their low numbers relative to keratins, melanosomes are approximately 10 times the diameter of the largest keratin structures in the epidermis⁵⁶ and possess a greater refractive index⁵⁷ (and therefore a greater difference in refractive index at their interface with skin). Melanin has been shown to contribute significantly to the degree of scatter within the epidermis.^{58,59} As well as the volume fraction, the distribution and size of melanin structures in the epidermis also vary with skin type. Thus, the total amount of scatter that occurs as a result of melanin in the epidermis can vary substantially between individuals,^{60,61} although this is not always taken into account when simulating the effects of varying melanin concentration on skin color,^{42,62} or when simulating laser treatments,^{15,63} for example.

Blood normally occupies around 0.2% to 0.6% of the physical volume of the dermis^{2,6,54,64–66} depending upon its anatomical location. The vessel walls surrounding this blood, in addition to the walls of vessels that remain vacant, may occupy a similar volume. Dermal vessels vary in thickness and structure from capillaries of around 10 to 12 μm diameter at the epidermal junction to terminal arterioles and post-capillary venules (approximately 25 μm in diameter) in the papillary dermis and venules (approximately 30 μm) in the mid-dermis.⁶⁷ Furthermore, blood vessels occur in higher densities at particular depths, giving rise to so-called blood vessel plexi.⁶⁷ The contribution to light scatter by these structures, inclusive of refraction effects, may be significant^{68–70} and varies with location and depth, as well as between individuals.* Larger, deeper vessels may also contribute to the color of skin.

*Assuming a reduced scattering coefficient of 0.5 mm^{-1} for blood and 40 mm^{-1} for vessel walls at 633 nm, a 0.5% volume fraction of each contributes approximately 0.2 mm^{-1} to the dermal reduced scattering coefficient, measured at around 1–5 mm^{-1} (Fig. 9). The contribution will be larger within blood vessel plexi.

Scattering from the remaining structures of the skin, including cell walls, nuclei, and organelles,³⁶ hairs and glands, is rarely of central interest to a study of skin optics. As a result, the contributions from these structures to the total measured scattering coefficients are not routinely considered separately.⁷¹

3 Simulating Light Transport Through Skin

Optical simulations involving mathematical models of healthy human skin generally approximate the surface as perfectly smooth, although some computer graphics models have applied calculations of directional reflectance from rough surfaces.⁷² Surface scattering effects (reflection and refraction) can be calculated for smooth surfaces using Fresnel's equations and Snell's law, respectively:

$$R = \frac{1}{2} \frac{(a - c)^2}{(a + c)^2} \left\{ 1 + \frac{[c(a + c) - 1]^2}{[c(a - c) + 1]^2} \right\}. \quad (1)$$

Fresnel reflection (R) of unpolarized light from air to skin, where $c = \cos(\theta_t)$, θ_i is the angle of incidence, $a = n^2 + c^2 - 1$ and n is the refractive index of skin.

$$\theta_t = \arcsin\left(\frac{1}{n} \sin \theta_i\right). \quad (2)$$

Angle of refraction (θ_t) at the skin's surface calculated using Snell's law.

Within the skin, both absorption and scatter must be considered simultaneously. These may be described in the classical approach by Maxwell's equations, which consider the interactions between the electric and magnetic fields of light with matter. However, an exact solution to Maxwell's equations requires precise knowledge of each structure within the medium and becomes prohibitively complex for the case of human skin.

The most commonly used approximation to Maxwell's equations in the field of skin optics is radiative transfer theory (RTT).⁷³ This considers the transport of light in straight lines (beams), with absorption simulated as a reduction in the radiance of a beam and dependent upon the absorption coefficient (μ_a). The degree of scattering is described by the scattering coefficient (μ_s), which considers both a loss of radiance in the direction of the beam and a gain from beams in other directions, and the phase function (p), the probability that an individual beam will scatter in any particular direction. The reduced-scattering coefficient (μ'_s) combines these variables, i.e., $\mu'_s = \mu_s(1 - g)$, where g is the anisotropy factor, the average cosine of the scattering angle θ :

$$g = \int_{4\pi} p(\cos \theta) \cos \theta d\omega, \quad (3)$$

where $d\omega$ is a differential solid angle.

In order for RTT to be valid, it must be assumed that any cause for increasing or decreasing the radiance of a beam other than that described by the absorption and scattering coefficients, including inelastic scatter (fluorescence or phosphorescence) and interactions between beams (interference), is negligible. The skin model must also consist of volumes that are homogeneous with regards to μ_s , μ_a and p , and that do not change over time.

4 Optical Coefficients of Skin

A considerable amount of work has been carried out to determine appropriate values of the RTT coefficients. Cheong et al.⁷⁴ described both direct (*in vitro*) and indirect (*in vivo*) methods of measuring absorption and scatter. A comprehensive analysis of the literature involving each method is presented here.

4.1 Absorption Coefficients

4.1.1 *In vitro* absorption coefficients

Direct measurements have the potential to produce repeat measurements of a predetermined volume or section of skin and, unlike *in vivo* measurements, can include transmission data. However, the processes necessary to extract and prepare a skin sample cannot be carried out without altering its optical properties.

The *in vitro* studies presented in Fig. 3 vary significantly in tissue-processing methodologies, measurement setup and the interpretation of data. For example, Jacques et al.'s work⁷⁵ included three methods of tissue preparation. The epidermis was separated from the dermis using a micro-cryotome for one set of skin samples, after mild thermal treatment in a water bath in another set, and was not separated in a third set. The same mild thermal treatment was used to separate the dermis and epidermis in Prah's work⁵⁵ and a micro-cryotome was also applied in Salomatina et al.'s study.⁵⁹ No separation of the epidermis was reported by Chan et al.⁷⁶ or Simpson et al.⁷⁷ Although Salomatina's work shows greater absorption from the *in vitro* epidermis when compared to the dermis, the studies analyzed here do not demonstrate a clear distinction in absorption coefficients reported between the methods of separation described, nor between those that separated the epidermis and those that did not.

The level of hydration is likely to have varied considerably between the studies analyzed. Prah⁵⁵ and Jacques et al.⁷⁵ soaked samples in saline for at least 30 min before carrying out measurements, during which the samples were placed in a tank of saline. Salomatina et al.⁵⁹ also soaked their skin samples prior to measurement and sealed them between glass slides to maintain hydration. Chan et al.⁷⁶ and Simpson et al.⁷⁷ did not soak their samples prior to or during measurement. Jacques et al. reported that soaking the sample increases back-scattered reflectance, although the effects on the calculated absorption are not described. Chan et al. commented that dehydration may elevate the measured absorption coefficient. However, the greatest reported absorption coefficients are those from rehydrated tissue samples. From the information available, the effect of tissue hydration on the measured absorption coefficients is not clear.

Data was interpreted using Monte Carlo simulations by Salomatina et al.,⁵⁹ Simpson et al.⁷⁷ and Graaf et al.,⁷⁸ an adding-doubling technique by Prah et al.,⁵⁵ and by direct interpretation in Chan et al.'s⁷⁶ and Jacques et al.'s⁷⁵ studies. Both the methods described in the Monte Carlo simulations and Prah's adding-doubling technique are based upon assumptions of optically homogeneous tissue layers, uniform illumination and no time dependence, and both are essentially discrete solutions to the radiative transport equation. The methods described contrast in their approach to internal reflection for beams exiting the skin model and the adding-doubling method relies upon accurate representation of the angular distribution of beams exiting the thin layer upon which the model is built. It is not directly

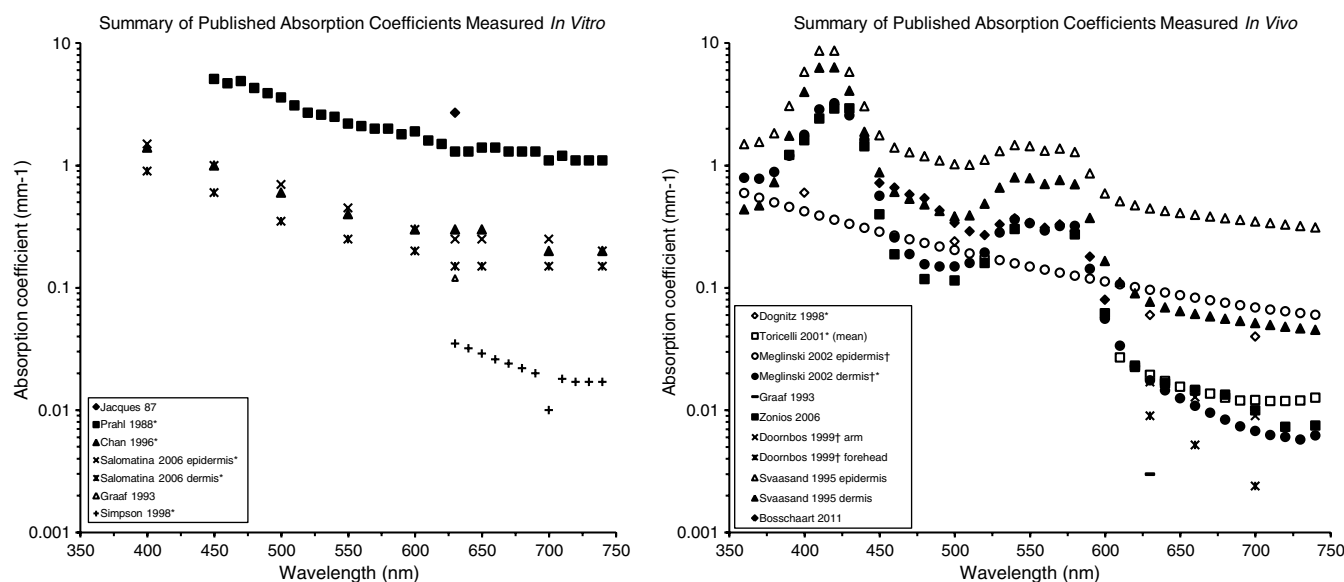


Fig. 3 Summary of absorption coefficients available in the literature. *In vitro* data represents absorption coefficients from exsanguinated skin whereas dermal *in vivo* data is inclusive of blood absorption. *Data obtained from graphical presentation. †Data presented was not complete and required input of hemoglobin or water optical properties obtained from.³⁵ The raw data is provided in the Appendix (Table 1).

clear if or how these differences may have contributed to the higher absorption coefficients reported by Prahl et al.

It is also of interest that Prahl et al.'s,⁵⁵ Chan et al.'s⁷⁶ and Salomatina et al.'s⁵⁹ studies, whose samples varied in thickness between 60 and 780 μm , did not demonstrate a clear correlation between sample thickness and published absorption coefficients but Simpson et al.'s published absorption coefficients, which are an order of magnitude smaller than the other values analyzed here, involved much thicker samples (1500 to 2000 μm thick). Thus, differences between the published absorption coefficients across these studies may have resulted from variations in the regions of skin investigated or the ability of the simulations to correctly account for boundary effects at the lower boundary.

4.1.2 *In vivo* absorption coefficients

Indirect measurements do not suffer from such changes in the properties of the interrogated skin volume, although care must be taken to consider variations in blood perfusion, for example, which may result from sudden changes in ambient temperature, the use of some drugs and even contact between the skin and the measurement device.⁷⁹

In general, absorption coefficients measured *in vivo* may be expected to be higher than *in vitro* values where the highly absorbing pigments from blood are removed from the samples. This is particularly true in the blue-green regions of the visible spectrum. Assuming a value of 0.5% blood volume in the dermis, this would contribute approximately 8 cm^{-1} at 410 nm (Soret band), 0.6 cm^{-1} at 500 nm and 1.4 cm^{-1} at 560 nm (*Q*-band), but only around 0.05 cm^{-1} at 700 nm (values calculated from³⁵). This contribution is not reflected in the literature. Absorption coefficients obtained from *in vivo* work show greater variation, but are not consistently higher than those obtained from *in vitro* work (Fig. 3).

Absorption coefficients from Svaasand et al.,⁸⁰ Zonios et al.,⁸¹ and Meglinski and Matcher⁴² clearly demonstrate the effect of blood on the measured absorption coefficients. Each

study shows an absorption peak between 400 and 450 nm corresponding to the Soret band and a double peak at approximately 540 and 575 nm corresponding to the α and β bands of oxyhemoglobin (see Fig. 1). There are, however, notable differences between the absorption coefficients produced from the three studies. Meglinski and Matcher and Svaasand et al. considered epidermal absorption coefficients separately to dermal values. The reported values from Svaasand et al. are greater, and show a different spectral curve to those from Meglinski and Matcher. This is a direct result of Svaasand et al.'s inclusion of 0.2% blood by volume in the calculation of epidermal absorption coefficients, representing blood infiltrating the modeled epidermal layer from the papillae. Compared to Meglinski and Matcher's dermal values and Zonios et al.'s absorption coefficients for their skin model consisting a single layer, both of which also included the influence of blood, Svaasand et al.'s reported dermal absorption coefficients were consistently high. This is despite using a dermal blood volume fraction of 2%, compared to an average of 12% from Meglinski and Matcher's study and a value of 2.6% in Zonios et al.'s work. The cause of this discrepancy is the variation in magnitude of the blood absorption coefficients applied across the three studies (Fig. 6, Appendix). Bosschaart et al.⁸² employed a diffusion approximation technique to their data collected from neonates, effectively applying a single value of absorption across the skin volume. Their data is in close agreement to Meglinski and Matcher's dermal absorption coefficients in the 530- to 600-nm range, but the contribution of melanin produces a relative increase in Bosschaart et al.'s values at shorter wavelengths.

Data selected for analysis in this work involved "Caucasian" skin types only. Where stated, these studies involved skin types described as Northern European. Where not stated, it was assumed that such skin types were used except for the studies carried out by Zonios et al.⁸¹ and Torricelli et al.⁸³ that were conducted in Southern Europe. However, the latter two studies did not report higher absorption coefficients, as may be expected from measurements on darker skin types. In Zonios et al.'s

work, this is primarily a result of the low values of blood absorption coefficient applied. Torricelli et al.⁸³ was the only group to apply time-resolved reflectance spectroscopy. This involves a prediction of the temporal spread of a laser pulse using a diffusion model. The values presented can only be as good as the diffusion model, and rely upon a wavelength dependence determined from phantom measurements.⁸⁴

The absorption coefficients from both Graaf et al.'s⁷⁸ and Doornbos et al.'s⁸⁵ studies were lower than those from the remaining studies. Both studies involved an integrating sphere and multifiber probe, respectively, as did the higher values from Svaasand et al.⁴⁰ and Meglinski and Matcher.⁴² Graaf et al. and Doornbos et al. applied a Monte Carlo Simulation and diffusion approximation respectively, as did Meglinski and Matcher and Svaasand et al. The multiple layered mathematical skin models that Svaasand et al. and Meglinski and Matcher applied when separately considering the effects of the epidermis and dermis may be a more accurate approach than the single homogeneous layer used in Graaf et al.'s and Doornbos et al.'s work. Although the cause of lower values is not clear, Graaf et al. commented that their absorption coefficient at 633 nm was "much smaller than expected from *in vivo*" results. Doornbos et al. did not comment directly on the cause of their low values, but mentioned that their "results resemble those of Graaf et al."

4.2 Scattering Coefficients

4.2.1 *In vitro* scattering coefficients

Of the studies analyzed here, both Prahl's⁵⁵ and Jacques et al.'s⁷⁵ studies describe a number of processes between tissue extraction and measurement that are likely to have had an effect on the measured reduced-scattering coefficient, including: exposure to a 55°C water bath for 2 min to aid with separating the epidermis from the dermis; freezing, cutting and stacking of 20- μ m thick slices of the dermis; and soaking in saline to rehydrate and wash away any blood. The bloodless samples were then held

between glass slides in a saline-filled tank and illuminated using a 633-nm laser. Freezing and drying, heating to remove the epidermis and deformation of skin samples have all been reported to change the measured values of scattering and absorption coefficients.^{75,77,78} In particular, experimental work by Pickering et al.⁸⁶ suggested that heating tissue to 55°C may increase the value of μ_s . Also, Jacques et al.⁷⁵ commented that soaking the dermis (in saline) will increase the backscattered reflectance, and thus may increase the calculated scattering coefficient. In contrast, Chan et al.⁷⁶ and Simpson et al.,⁷⁷ whose reduced-scattering coefficients were substantially lower, reported minimal tissue processing (although Chan et al.'s specimens had previously been frozen).

A further source of disparity between *in vivo* data from earlier studies,^{55,75,78} which involved more tissue processing than the more recent *in vivo* data presented in Fig. 4,^{59,76,77} may have come from the choice of measurement setup. For example, Graaf et al.⁷⁸ reported that discrepancies may arise when internal reflectance is not taken into consideration. Due to a larger difference in refractive indices, this will have a greater effect for samples in air compared to samples in water or saline solution. All samples were placed between glass slides. However, only the earlier studies analyzed here, those which produced higher values of reduced-scattering coefficient, submerged the sample in water or saline.^{55,75}

Salomatina et al.'s study⁵⁹ determined separately the reduced-scattering coefficients of the epidermis and dermis. Their data show that the epidermal reduced-scattering coefficient was consistently 2 to 3 mm⁻¹ higher than the dermal reduced-scattering coefficient over the visible spectrum. This suggests that studies that excluded the epidermis, such as Chan et al.'s⁷⁶ and Simpson et al.'s,⁷⁷ should provide lower values of reduced-scattering coefficient than data obtained from studies in which the epidermis remained, such as Graaf et al.'s⁷⁸ and Prahl's.⁵⁵ However, most probably due to a prevailing effect from the aforementioned influences, this is not the case.

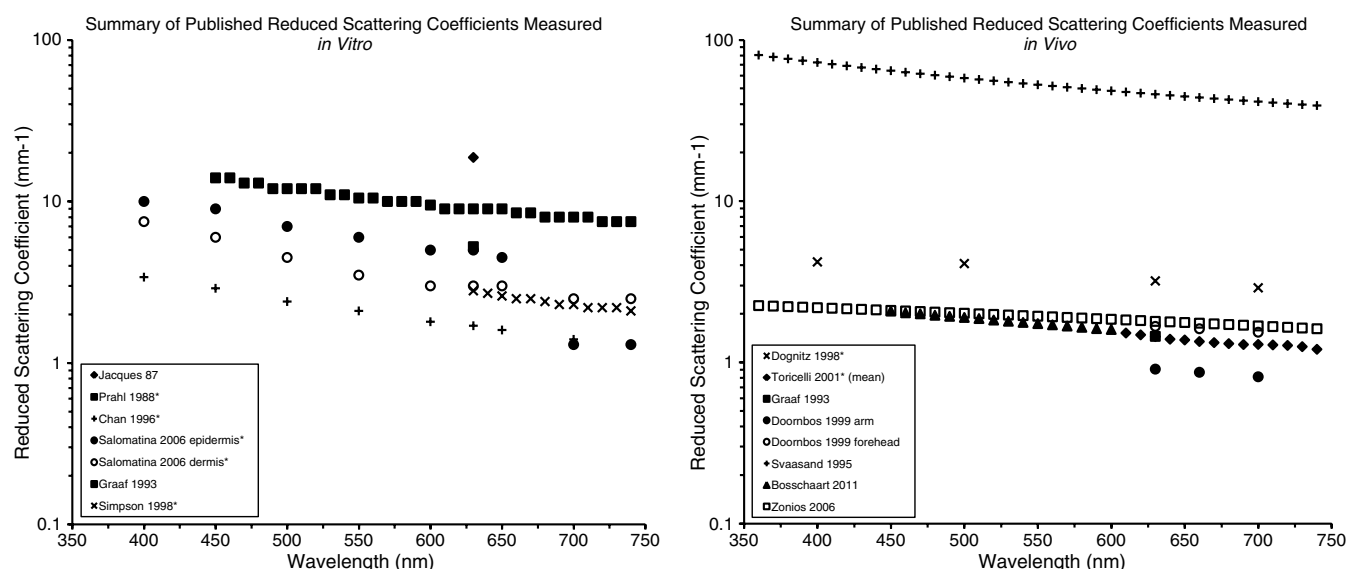


Fig. 4 Summary of reduced- scattering coefficients available in the literature. *In vitro* data represents absorption coefficients from exsanguinated skin whereas dermal *in vivo* data is inclusive of blood absorption. *Data obtained from graphical presentation. †Data presented was not complete and required input of hemoglobin or water optical properties obtained from Ref. 35. Raw data is provided in the Appendix (Table 2).

4.2.2 *In vivo* scattering coefficients

In addition to their interpretation of Prah1's *in vitro* data,⁵⁵ Graaf et al.⁷⁸ performed measurements of reflection on five male subjects with "white" skin at 660 nm using an LED source. Despite using a similar wavelength light source to Prah1's 633 nm, reduced-scattering coefficients from Graaf et al.'s *in vivo* measurements were appreciably lower than their interpretation of *in vitro* data (Fig. 4). This is likely to be a result of the posthumous tissue processing performed in Prah1's study as previously described. However, this effect is not reflected across the literature, as in general reduced-scattering coefficients from *in vivo* studies were not substantially lower than those evaluated from *in vitro* studies, nor did they demonstrate an appreciable difference when considering the variation in reduced-scattering coefficients across the visible spectrum.

Any solution involving two independent variables (such as μ'_s and μ_a) can suffer from nonuniqueness, where equivalent results can be obtained from two or more sets of input values (local minima). When applying RTT to skin, a simulated increase or reduction in reflection can be attributed to a change in either μ_a or μ'_s . The reduced-scattering coefficients from Svaasand et al.'s study⁴⁰ were considerably higher than any of the other *in vivo* studies assessed. This is in addition to their high values of absorption coefficient discussed in the previous section. The paper stated that "the fact that the calculated [skin reflectance] values tend to be higher than the measured ones might indicate that the used values for the epidermal and dermal (reduced) scattering coefficients are somewhat too high." The reduced-scattering coefficient from Svaasand et al.'s work was derived from a single data point at 577 nm measured by Wan et al.⁸⁷ fitted to a simple $\mu'_s \propto \text{wavelength}^{-1}$ relationship and therefore may not be as reliable as data derived from a series of direct measurements. It should also be noted that the remaining studies that produced the highest reduced-scattering coefficients analyzed here also provided the highest absorption coefficients, including both *in vivo* and *in vitro* data. Similarly, those studies presenting the lowest reduced-scattering coefficients produced the lowest absorption coefficients (Fig. 4). Furthermore, when applying high values of dermal scattering to a minimization procedure, Verkrusye et al. demonstrated the effect of nonuniqueness errors on derived skin properties, resulting in a clear overestimation of dermal blood volume fractions.⁴¹

Dognitz et al.⁸⁸ used a spatial frequency domain reflectometry (SFDR) method alongside a simulation constructed using the Wang and Jacques Monte Carlo program⁸⁹ to calculate reduced-scattering coefficients from the forearms of six subjects with Caucasian skin. Dognitz et al. commented that due to the differences in measurement techniques their method interrogates a more superficial region of tissue than reflectance spectroscopy (as used in the work by Graaf et al.,⁷⁸ Svaasand et al.⁴⁰ and Doornbos et al.⁸⁵) as there is no separation between source and detector. Salomatina et al.'s *in vitro* results demonstrate epidermal reduced-scattering coefficients that are greater than dermal values,⁵⁹ suggesting that studies involving SFDR may expect an increase in measured reduced-scattering coefficients compared to studies involving reflectance spectroscopy. Dognitz et al. further commented that discrepancies due to surface reflection may cause their method to overestimate the reduced-scattering coefficient. These comments are supported elsewhere in the literature⁹⁰ and by the remaining data sets that (with

the exception of Svaasand et al.'s work) demonstrate good agreement.

Other techniques used to assess reduced-scattering coefficients include Torricelli et al.'s time-resolved reflectance spectroscopy,⁸³ Bosschaart et al.'s diffusion approximation technique⁸² and a Mie theory calculation by Zonios et al. that included spherical scatterers with Gaussian distribution in size.^{81,91} The results from these studies are consistent with the majority of *in vivo* studies and with those *in vitro* studies that reported minimal tissue processing.

4.3 Further Causes of Discrepancy in the Absorption and Scattering Coefficients

It may be the case that the primary cause of discrepancy between the studies analyzed here is a result of true differences between the skin samples selected. The degree to which such differences influence the measured coefficients is difficult to extract, as to the authors' knowledge, there are no studies that involve the measurement of optical properties from large numbers of skin samples, and none that determine the expected variation between samples with any one method of data acquisition or interpretation. Of the studies reviewed, the largest datasets involving a single measurement technique involved six subjects (one involved a range of skin types,⁴⁰ the other used three male and three female subjects⁸⁰). Only the former study commented on the variation between individuals, with darker skin types demonstrating greater absorption across the visible spectrum. However, measurements were carried out on only one or two subjects from each skin type and the difference in epidermal scattering due to variations in melanin content was not considered.

Further variations between published absorption and scattering coefficients may have been caused by differences in the interpretation of data. Perhaps the most widely referenced set of absorption and scattering data for human skin is that published by Jacques et al.⁷⁵ Interpretation of the acquired data was carried out using the diffusion approximation. Prah1, who was an author of this paper, presented an almost identical process for determining the optical properties of abdominal skin samples in his PhD thesis⁵⁵ but applied a technique described as an "adding-doubling" method. This is a one-dimensional (1-D) iterative technique that uses RTT to estimate the transport of light through skin from the reflection and transmission of two or more mathematical "slabs."^{55,92} Graaf et al.⁷⁸ provided a further analysis of Prah1's data⁵⁵ using a Monte Carlo technique. The absorption coefficients calculated across these studies varied from 0.12 to 0.27 mm⁻¹ and the reduced-scattering coefficients from 5.3 to 18.7 mm⁻¹ at 633 nm. This demonstrates that an alternative analysis of the same data can lead to a wide range in estimates of optical coefficients.

Van Gemert et al.⁹³ used a diffusion theory model to compare absorption and scattering coefficients from a compilation of *in vitro* measurements including Jacques et al.'s study⁷⁵ and papers published elsewhere.^{50,87,94} Despite applying the same method of interpretation for each data set, dermal absorption and scattering coefficients varied at 633 nm by a factor of nearly 2.5 (approximately 0.18 to 0.43 mm⁻¹ and 1.8 to 4.1 mm⁻¹, respectively). Hence, not only do alternative analyses provide noticeable differences in reported coefficients, but the same analysis of data from similar studies shows that there is a considerable difference in calculated coefficients across the published data.

4.4 Phase Functions

By far the most widely used approximation to the phase function of human skin is that first used by Henyey and Greenstein when trying to model diffuse radiation in the Milky Way galaxy.⁹⁵ The principal benefit of applying the Henyey-Greenstein (HG) phase function is that it can be described using only a single parameter, the modified anisotropy factor, g_{HG} .

$$p(\cos \theta) = \frac{1 - g_{\text{HG}}^2}{2(1 + g_{\text{HG}}^2 - 2g_{\text{HG}} \cos \theta)^{3/2}}. \quad (4)$$

A number of investigations have been conducted to determine the validity of the HG phase function when applied to human skin. For example, Mourant et al.⁴⁶ used a goniometer setup to measure the phase function of cell suspensions *in vitro* and Dunn and Richards-Kortum⁹⁶ simulated scattering from an individual cell using a finite difference time domain simulation.[†] Both studies found that the HG function was a poor approximation to the scattering from individual cells as it underestimates scattering at large angles, although Mourant et al. commented that the HG phase function reproduces the experimentally measured phase function “reasonably well for angles less than 75 deg.” This is in agreement with other work.^{97–100}

In order to compensate for the weaknesses in nonforward scattering, Jacques et al.⁷⁵ introduced an additional empirical term representing the proportion of isotropic scattering. They performed goniometric measurement of scattered light through tissue samples and fitted the data to the modified HG function (Eq. 5).

$$p(\cos \theta) = \frac{1}{2} \left[b + (1 - b) \frac{1 - g_{\text{mod}}^2}{2(1 + g_{\text{mod}}^2 - 2g_{\text{mod}} \cos \theta)^{3/2}} \right], \quad (5)$$

where $g_{\text{mod}} = \int_{4\pi} p(\cos \theta) \cos \theta d\omega'$ and where b is the proportion of isotropic scattering. Applying a value of $b = 0.1$, they calculated $g_{\text{mod}} = 0.82$ at 633 nm. Van Gemert et al.⁹³ and Sharma and Banerjee¹⁰¹ supported the use of this modified HG phase function when comparing results to *in vitro* goniometer measurements and Monte Carlo simulations respectively. Furthermore, Graaf et al.⁴⁸ reported that the value of the anisotropy factor used in Jacques et al.'s study was in agreement with a Mie scattering model of a set of spherical scattering particles with radius of 0.37 μm .

The Henyey-Greenstein expression is purely empirical, however the Mie phase function is derived from a mechanistic theory of light transport and can be used to accurately determine the phase function from a single spherical particle. Several authors have attempted to justify the use of Mie theory calculation for the phase function within specified volumes of a skin model.^{60,102,103} However, calculations require adequate knowledge of the sizes and refractive indices of scattering particles within the skin and are complex when considering a distribution of these parameters. Although such calculations are possible,¹⁰⁴ they have not been shown to offer significant advantages over the conventional HG phase function.

The FDTD method used by Dunn and Richards-Kortum⁹⁶ and Mourant⁴⁶ was capable of predicting the effects of cell structures on the scattering phase function for a single cell, including nuclei and melanin, but did not offer a comparison with measured skin data. Liu¹⁰⁵ introduced a new phase function in an attempt to improve upon the HG phase function. This study concluded that the new phase function showed better agreement to a Mie calculation when compared to a HG phase function. Again, no direct comparison to measured skin data was presented.

4.5 Refractive Indices

The surface of the skin is usually approximated as perfectly smooth and thus simulations of surface scatter depend entirely upon an input of refractive index. Ding et al.¹⁰⁶ illuminated the skin *in vitro* using a number of light sources ranging in wavelength from 325 to 1557 nm. By fitting their data to dispersion schemes used previously on ocular tissues, they predicted values of refractive index ranging from approximately 1.41 to 1.49 in epidermal tissues and 1.36 to 1.41 in dermal tissues over the wavelength range. This is in agreement with other data published using an equivalent technique.^{107,108} However, Tearney et al.'s study¹⁰⁹ applied Optical Coherence Tomography to measure refractive indices of *in vivo* skin at 1300 nm and determined values from a single participant of 1.52 for the stratum corneum, 1.34 for the living epidermis and 1.41 for the dermis. Considering the aforementioned influence of posthumous tissue processing on measured reduced-scattering coefficients, it may also be the case that refractive indices are similarly affected. Comparing Tearney et al.'s *in vivo* refractive indices to Ding et al.'s *in vitro* values (1.46 for the combined epidermis and stratum corneum and 1.36 for the dermis at 1300 nm), there is a suggestion that *in vitro* methods may result in an increase in the measured refractive indices.

4.6 Blood and Blood Vessels

The optical properties of blood differ from those of other tissues within skin as blood does not contain significant intercellular scatterers. Thus, the optical properties of blood are primarily determined from the concentration and distribution of erythrocytes. Although a number of investigations have been carried out on human blood, many have used agitated vials containing randomly distributed and oriented erythrocytes that are not representative of blood as it appears in the dermis.^{110,111} Changes in erythrocyte organization, shape and orientation have all been shown to influence the optical properties of blood flowing within vessels.¹¹⁰ Only two studies were found that have attempted to measure the optical properties of flowing blood.^{112,113} Although the results from these two studies are not in complete agreement, they both suggest that blood exhibits increased absorption and decreased scattering relative to remaining skin, with a reduced-scattering coefficient and absorption coefficient of flowing blood of around 2.5 mm^{-1} and 0.5 mm^{-1} , respectively, at a wavelength of 633 nm.

To the authors' knowledge, the optical properties of dermal blood vessel walls have not been investigated directly. However, studies of scatter from aortic walls suggest a scattering coefficient of around 40 mm^{-1} at 600 nm,¹¹⁴ which appears to be greater than the surrounding dermis (Fig. 4). Surface scattering (as estimated using refractive indices) is also of particular importance when considering blood vessels in the skin (Fig. 5).

[†]A direct solution of Maxwell's equations in the time domain.

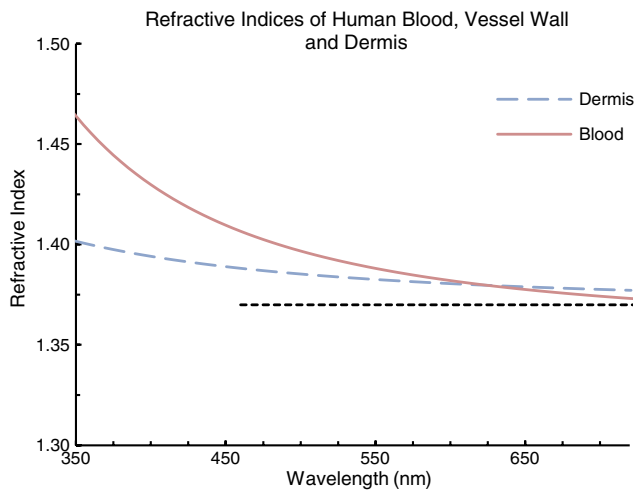


Fig. 5 Refractive indices of human blood,¹¹⁵ vessel wall^{116,117} and dermis.¹¹⁸

It can be seen in Fig. 5 that the reported refractive indices of the vessel wall, blood and surrounding dermis are similar in the yellow to red regions (>550 nm) but differ significantly at the blue to violet end. Thus, greater scattering (reflection and refraction) will occur at the vessel wall at shorter wavelengths within the visible spectrum. It may be of interest to note that the scattering effects described here further contribute to the green/blue appearance of larger vessels in the skin.

Although studied,^{119,120} the HG phase function has not been substantially supported for the approximation of *in vivo* blood scattering anisotropy in skin. At present, analytical methods have more success in this case.^{111,121}

5 Conclusion

Light transport through skin is dependant both upon the effects of scattering structures such as filamentous proteins, and upon the quantity and distribution of highly absorbing chromophores such as melanin and hemoglobin. Simulations of these effects are most commonly achieved using RTT.

Orders of magnitude variation were found to exist between RTT absorption and scattering coefficients across the literature. Absorption coefficients were found to be profoundly affected by the presence of blood, as demonstrated when comparing *in vitro* to *in vivo* data, and reduced-scattering coefficients demonstrated a clear increase in magnitude resulting from tissue processing of *in vitro* samples. Fewer studies were found that analyzed anisotropy factors and refractive indices, or that considered directly the optical properties of dermal blood vessels.

Due to the known effects of tissue processing on reduced-scattering coefficients and the unavoidable coupling between absorption and scatter on measurements on *in vivo* skin, *in vitro* scattering coefficients that report minimal tissue processing, such as the study by Chan et al.⁷⁶ should be considered foremost in future studies of skin optics. The effect of blood on the reported absorption coefficients, along with the observed coupling effects between absorption and scatter, suggest lower values of absorption coefficients measured *in vivo*, such as those reported by Meglinski and Matcher⁴² or Zonios et al.,⁸¹ appear to be the most reliable choice. The HG phase function has a

proven track record in skin optics, but published values of anisotropy factor and refractive indices are too few to provide a thorough comparison.

The analysis of the literature regarding the optical properties of skin presented here clearly demonstrates the need for further studies involving larger numbers of patients to establish a definitive range of realistic coefficients for clinically normal skin over a range of skin types.

Appendix

This appendix provides the values used for the analysis of absorption (Table 1) and reduced-scattering coefficients (Table 2) reported in the literature, while * denotes values obtained from graphical presentations. The remaining data was extracted directly from the text or tables of the publications unless otherwise stated below.

A.1 Absorption Coefficients

Meglinski and Matcher's calculated absorption coefficients were presented separately for the dermis and epidermis. Epidermal absorption coefficients were calculated using Meglinski and Matcher's Eq. (14)⁴² with the following inputs: $C_{\text{melanin}} = 2.0\%$, $C_{\text{H}_2\text{O}} = 20\%$, $\mu_a^{(0)} = (7.84 \times 10^6) \lambda^{-3.225}$ [Eq. (10) in their paper and from Ref. 122], $\mu_a^{\text{melanin}} = (5 \times 10^9) \lambda^{-3.33}$ and taken from Ref. 35. The dermal absorption coefficients were calculated separately for the papillary layer, upper and lower blood net layers and the reticular dermis using the concentration and blood and water presented in their Table 2, value of $\mu_a^{\text{H}_2\text{O}}$ taken from Ref. 35, and values of μ_a^{Hb} and $\mu_a^{\text{HbO}_2}$ also taken from Ref. 35.

Svaasand et al.'s epidermal and dermal absorption coefficients were calculated from their Eq. (6), with values of μ_{ab} calculated using their Eq. (2). Values of μ_{an} were calculated from Ref. 122, and a value of $\mu_{am,694} = 0.3 \text{ mm}^{-1}$ corresponding to Caucasian skin (see their Fig. 3). Epidermal and dermal blood volume fractions of 0.2% and 2% were applied to the epidermal and dermal layers, respectively.

Zonios et al.'s absorption coefficients were calculated from their Eq. (18) using parameters of melanin and absorption concentrations, as well as blood oxygen saturation, presented in their Table 2. The paper by Zonios et al. did not describe the origin of the hemoglobin and oxyhemoglobin extinction coefficients applied in their study, thus it was assumed that values taken from Ref. 123 were used, as was the case in a previous paper by Zonios et al.⁹¹

The blood absorption coefficients used in these three studies are presented in Fig. 6 for comparison.

A.2 Reduced-Scattering Coefficients

Torricelli et al.'s study presented separate datasets for the arm, head and abdomen from three participants. The mean of these nine values for each wavelength, determined from graphical data, is presented here. Equation (3) from Svaasand et al.'s work and Eq. (19) from Zonios et al.'s work were used to calculate the values presented in the Appendix. Zonios et al.'s Eq. (19) required inputs of d_0 , d_s and μ_s' that were selected as normal skin values from Zonios et al.'s paper as $0.0625 \mu\text{m}$, $0.49 \mu\text{m}$ and 2.1 mm^{-1} , respectively.

Wavelength (nm)	In vitro absorption coefficients (mm ⁻¹)				In vivo absorption coefficients (mm ⁻¹)										Zonios 2006	Bosschaart 2011
	Prahl 1988*	Chan 1996*	Salomatina 2006 epidermis*	Salomatina 2006 dermis*	Graaf 1993	Simpson 1998*	Dognitz 1998*	Torricelli 2001* (mean)	Meglinski 2002 epidermis [†]	Meglinski 2002 dermis [†] *	Graaf 1993	Doornbos 1999 [†] arm	Doornbos 1999 [†] forehead	Svaasand 1995 epidermis		
360									0.60	0.79				1.50	0.41	
370									0.55	0.78				1.56	0.41	
380									0.50	0.89				1.84	0.52	
390									0.46	1.20				3.07	1.02	1.22
400		1.4	1.5	0.9			0.6		0.42	1.78				5.83	2.13	1.61
410									0.39	2.88				8.68	3.27	2.42
420									0.36	3.23				8.68	3.28	2.92
430									0.33	2.57				5.84	2.15	2.93
440									0.31	1.62				3.05	1.04	1.44
450	5.1	1	1	0.6					0.29	0.566				1.77	0.53	0.40
460	4.7								0.27	0.258				1.40	0.39	0.19
470	4.9								0.25	0.189				1.28	0.35	0.58
480	4.3								0.23	0.156				1.19	0.31	0.12
490	3.9								0.22	0.149				1.10	0.28	0.43
500	3.6	0.6	0.7	0.35			0.24		0.20	0.150				1.03	0.26	0.11
510	3.1								0.19	0.160				1.01	0.26	0.29
520	2.7								0.18	0.194				1.11	0.30	0.16
530	2.6								0.17	0.283				1.31	0.38	0.33
540	2.5								0.16	0.362				1.47	0.45	0.30
550	2.2	0.4	0.45	0.25					0.15	0.338				1.44	0.44	0.34
560	2.1								0.14	0.294				1.32	0.40	0.31

Table 1 (Continued).

Wavelength (nm)	In vitro absorption coefficients (nm ⁻¹)					In vivo absorption coefficients (nm ⁻¹)												
	Jacques 87	Prahl 1988*	Chan 1996*	Salomatina 2006 epidermis*	Salomatina 2006 dermis*	Graaf 1993	Simpson 1998*	Dognitz 1998*	Toricelli 2001* (mean)	Meglinski 2002 epidermis†	Meglinski 2002 dermis†*	Graaf 1993	Doornbos 1999† arm	Doornbos 1999† forehead	Svaasand 1995 epidermis	Svaasand 1995 dermis	Zonios 2006	Bosschaart 2011
570			2.0							0.13	0.320				1.37	0.42		0.33
580			2.0							0.13	0.321				1.29	0.39	0.27	0.29
590			1.8							0.12	0.143				0.86	0.22		0.18
600			1.9	0.3	0.3	0.2				0.11	0.056				0.59	0.12	0.06	0.08
610			1.6						0.027	0.11	0.034				0.51	0.09		
620			1.5						0.023	0.10	0.023				0.47	0.08	0.02	
630	2.7		1.3	0.3	0.25	0.15	0.12	0.035	0.06	0.10	0.018	0.003	0.017	0.009	0.45	0.07		
640			1.3					0.032		0.09	0.015				0.42	0.06	0.02	
650			1.4	0.3	0.25	0.15		0.029	0.016	0.09	0.013				0.41	0.06		
660			1.4					0.026	0.015	0.08	0.011		0.013	0.005	0.40	0.06	0.01	
670			1.3					0.024	0.014	0.08	0.010				0.38	0.05		
680			1.3					0.022	0.013	0.08	0.008				0.37	0.05	0.01	
690			1.3					0.02	0.012	0.07	0.007				0.36	0.05		
700			1.1	0.2	0.25	0.15	0.01	0.04	0.012	0.07	0.007		0.009	0.002	0.35	0.05	0.01	
710			1.2				0.018		0.012	0.07	0.006				0.34	0.05		
720			1.1				0.017		0.012	0.06	0.006				0.33	0.04	0.01	
730			1.1				0.017		0.012	0.06	0.006				0.32	0.04		
740			1.1	0.2	0.2	0.15	0.017		0.013	0.06	0.006				0.31	0.04	0.01	

Table 2 Reduced- scattering coefficients (mm^{-1}) available from the literature. Precision of recorded value is dependent upon the nature of the original values presented.

Wavelength (nm)	in vitro reduced- scattering coefficients (mm ⁻¹)					in vivo reduced- scattering coefficients (mm ⁻¹)									
	Jacques 87	Prahl 1988*	Chan 1996*	Salomatina 2006 epidermis*	Salomatina 2006 dermis*	Graaf 1993	Simpson 1998*	Dognitz 1998*	Torricelli 2001* [mean]	Graaf 1993	Doornbos 1999 arm	Doornbos 1999 forehead	Svaasand 1995	Zonios 2006	Bosschaart 2011
360													80.6	2.25	
370													78.4	2.23	
380													76.3	2.22	
390													74.4	2.20	
400			3.4	10	7.5			4.2					72.5	2.18	
410													70.7	2.17	
420													69.0	2.15	
430													67.4	2.13	
440													65.9	2.12	
450		14.0	2.9	9	6								64.4	2.10	2.08
460		14.0											63.0	2.08	2.03
470		13.0											61.7	2.07	2.00
480		13.0											60.4	2.05	1.96
490		12.0											59.2	2.03	1.93
500		12.0	2.4	7	4.5			4.1					58.0	2.02	1.90
510		12.0											56.9	2.00	1.87
520		12.0											55.8	1.98	1.83
530		11.0											54.7	1.97	1.80
540		11.0											53.7	1.95	1.77
550		10.5	2.1	6	3.5								52.7	1.93	1.74
560		10.5											51.8	1.92	1.71
570		10.0											50.9	1.90	1.68

Table 2 (Continued).

Wavelength (nm)	in vitro reduced- scattering coefficients (mm ⁻¹)					in vivo reduced- scattering coefficients (mm ⁻¹)					Zonios 2006	Bosschaart 2011			
	Jacques 87	Prahl 1988*	Chan 1996*	Salomatina 2006 epidermis*	Salomatina 2006 dermis*	Graaf 1993	Simpson 1998*	Dognitz 1998*	Tarricelli 2001* (mean)	Graaf 1993			Doornbos 1999 arm	Doornbos 1999 forehead	Svaasand 1995
580		10.0											50.0	1.88	1.65
590		10.0											49.2	1.87	1.62
600		9.5	1.8	5	3								48.3	1.85	1.60
610		9.0							1.52				47.5	1.83	
620		9.0							1.48				46.8	1.82	
630/633	18.73	9.0	1.7	5	3	5.25	2.8	3.2	1.44	1.45	0.91	1.67	46.0	1.80	
640		9.0					2.7		1.39				45.3	1.78	
650		9.0	1.6	4.5	3		2.6		1.38				44.6	1.77	
660		8.5					2.5		1.35		0.87	1.62	43.9	1.75	
670		8.5					2.5		1.33				43.3	1.73	
680		8.0					2.4		1.31				42.6	1.72	
690		8.0					2.3		1.29				42.0	1.70	
700		8.0	1.4	1.3	2.5		2.3	2.9	1.29		0.81	1.54	41.4	1.68	
710		8.0					2.2		1.28				40.8	1.67	
720		7.5					2.2		1.27				40.3	1.65	
730		7.5					2.2		1.25				39.7	1.63	
740		7.5	1.3	1.3	2.5		2.1		1.21				39.2	1.62	

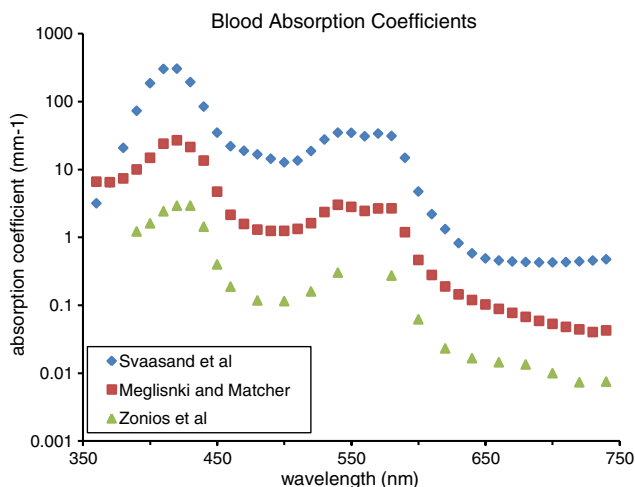


Fig. 6 Blood absorption coefficients used in three of the studies analyzed here.

References

1. T. S. Lister, P. A. Wright, and P. H. Chappell, "Spectrophotometers for the clinical assessment of port wine stain skin lesions: a review," *Lasers Med. Sci.* **25**(3), 449–457 (2010).
2. I. Nishidate, Y. Aizu, and H. Mishina, "Estimation of melanin and hemoglobin in skin tissue using multiple regression analysis aided by Monte Carlo simulation," *J. Biomed. Opt.* **9**(4), 700–710 (2004).
3. M. Shimada et al., "Melanin and blood concentration in a human skin model studied by multiple regression analysis: assessment by Monte Carlo simulation," *Phys. Med. Biol.*, **46**(9), 2397–2406 (2001).
4. D. Yudovsky and L. Pilon, "Rapid and accurate estimation of blood saturation, melanin content, and epidermis thickness from spectral diffuse reflectance," *Appl. Opt.* **49**(10), 1707–1719 (2010).
5. G. Zonios et al., "Melanin absorption spectroscopy: new method for noninvasive skin investigation and melanoma detection," *J. Biomed. Opt.* **13**(1), 014017 (2008).
6. W. Verkrusysse, G. W. Lucassen, and M. J. C. van Gemert, "Simulation of color of port wine stain skin and its dependence on skin variables," *Lasers Surg. Med.* **25**(2), 131–139 (1999).
7. I. Nishidate et al., "Visualizing depth and thickness of a local blood region in skin tissue using diffuse reflectance images," *J. Biomed. Opt.* **12**(5), 054006 (2007).
8. I. Nishidate et al., "Color appearance of skin tissues and blood vessels: in-vitro and in-vivo experiments," *Proc. SPIE* **4416**, 380–383 (2001).
9. Y. Aizu et al., "Spectrophotometric investigation of skin blood vessels on the basis of color perception," *Proc. SPIE* **3749**, 735–736 (1999).
10. A. Mazzoli, R. Munaretto, and L. Scalise, "Preliminary results on the use of a noninvasive instrument for the evaluation of the depth of pigmented skin lesions: numerical simulations and experimental measurements," *Lasers Med. Sci.* **25**(3), 403–410 (2010).
11. I. Hamzavi et al., "Spectroscopic assessment of dermal melanin using blue vitiligo as an in vivo model," *Photodermatol. Photoimmunol. Photomed.* **22**(1), 46–51 (2006).
12. L. L. Randeberg, E. L. Larsen, and L. O. Svaasand, "Characterization of vascular structures and skin bruises using hyperspectral imaging, image analysis and diffusion theory," *J. Biophotonics.* **3**(1–2), 53–65 (2010).
13. B. Stam et al., "3d finite compartment modeling of formation and healing of bruises may identify methods for age determination of bruises," *Med. Biol. Eng. Comput.* **48**(9), 911–921 (2010).
14. S. Nickell et al., "Anisotropy of light propagation in human skin," *Phys. Med. Biol.* **45**(10), 2873–2886 (2000).
15. M. J. C. van Gemert et al., "Non-invasive determination of port wine stain anatomy and physiology for optimal laser treatment strategies," *Phys. Med. Biol.* **42**(5), 937–950 (1997).
16. A. A. Strattonnikov et al., "Application of backward diffuse reflection spectroscopy for monitoring the state of tissues in photodynamic therapy," *Quantum Electron.* **36**(12), 1103–1110 (2006).
17. Y. Wang et al., "The change of reflection spectra and fluorescence spectra of port wine stains during pdt," *Spectros. Spectral Anal.* **31**(11), 2969–2972 (2011).
18. J. L. Sandell and T. C. Zhu, "A review of in-vivo optical properties of human tissues and its impact on pdt," *J. Biophotonics.*, **4**(11–12), 773–787 (2011).
19. M. Mehrubeoglu et al., "Skin lesion classification using oblique-incidence diffuse reflectance spectroscopic imaging," *Appl. Opt.* **41**(1), 182–192 (2002).
20. E. Salomatina et al., "Optical properties of normal and cancerous human skin in the visible and near-infrared spectral range," *J. Biomed Opt.* **11**(6), 064026 (2006).
21. V. P. Wallace et al., "Spectrophotometric assessment of pigmented skin lesions: methods and feature selection for evaluation of diagnostic performance," *Phys. Med. Biol.* **45**(3), 735–751 (2000).
22. J. Berg, J. Tymoczko, and L. Stryer, Chapter 7, "Hemoglobin: portrait of a protein in action," *Biochemistry*, 6th ed, pp. 183–194, WH Freeman, New York (2006).
23. J. A. Lukin et al., "Quaternary structure of hemoglobin in solution," *Proc. Nat. Academy Sci.* **100**(2), 517–520 (2003).
24. O. V. Kosmachevskaya and A. F. Topunov, "Hemoglobins: diversity of structures and functions," *Appl. Biochem. Microbiol.* **45**(6), 563–587 (2009).
25. J. R. Platt, "Visible and near-visible light," Chapter 2 in *Radiation Biology*, Vol. III, McGraw Hill, New York (1956).
26. M. C. Hsu and R. W. Woody, "Origin of the heme cotton effects in myoglobin and hemoglobin," *J. Am. Chem. Soc.* **93**(14), 3515–3525 (1971).
27. W. G. Zijlstra, A. Buursma, and W. P. Meeuwseenvanderroest, "Absorption-spectra of human fetal and adult oxyhemoglobin, de-oxyhemoglobin, carboxyhemoglobin, and methemoglobin," *Clin. Chem.* **37**(9), 1633–1638 (1991).
28. J. Riesz, "The spectroscopic properties of melanin," Ph.D. Thesis, University of Queensland (2007).
29. P. Meredith et al., "Towards structure-property-function relationships for eumelanin," *Soft. Matter.* **2**(1), 37–44 (2006).
30. E. Kaxiras et al., "Structural model of eumelanin," *Phys. Rev. Lett.* **97**(21), 218102 (2010).
31. K. Stepien et al., "Melanin from epidermal human melanocytes: study by pyrolytic gc/ms," *J. Am. Soc. Mass Spectrom.* **20**(3), 464–468 (2009).
32. G. Zonios and A. Dimou, "Melanin optical properties provide evidence for chemical and structural disorder in vivo," *Opt. Express* **16**(11), 8263–8268 (2008).
33. A. A. R. Watt, J. P. Bothma, and P. Meredith, "The supramolecular structure of melanin," *Soft. Matter.*, **5**(19), 3754–3760 (2009).
34. M. doi and S. Tominaga, "Spectral estimation of human skin color using the Kubelka-Munk theory," *Proc. SPIE* **5008**, 221–228 (2003).
35. S. A. Prah and S. L. Jacques, "Optical properties spectra," <http://omlc.org.edu/spectra/> (18 June 2009).
36. M. Bohnert et al., "A Monte Carlo-based model for steady-state diffuse reflectance spectrometry in human skin: estimation of carbon monoxide concentration in livor mortis," *Int. J. Legal Med.* **119**(6), 355–362 (2005).
37. J. B. Dawson et al., "A theoretical and experimental-study of light-absorption and scattering by in-vivo skin," *Phys. Med. Biol.* **25**(4), 695–709 (1980).
38. L. L. Randeberg et al., "A novel approach to age determination of traumatic injuries by reflectance spectroscopy," *Lasers Surg. Med.* **38**(4), 277–289 (2006).
39. S. Andree, J. Helfmann, and I. Gersonde, "Determination of chromophore concentrations from spatially resolved skin measurements," *Proc. SPIE* **8087**, 808716 (2011).
40. L. O. Svaasand et al., "Tissue parameters determining the visual appearance of normal skin and port-wine stains," *Lasers Med. Sci.* **10**(1), 55–65 (1995).
41. W. Verkrusysse et al., "A library based fitting method for visual reflectance spectroscopy of human skin," *Phys. Med. Biol.* **50**(1), 57–70 (2005).
42. I. V. Meglinski and S. J. Matcher, "Quantitative assessment of skin layers absorption and skin reflectance spectra simulation in the visible and near-infrared spectral regions," *Physiological Measurement.* **23**(4), 741–753 (2002).

43. R. R. Anderson and J. A. Parrish, "The optics of human skin," *J. Invest. Dermatol.* **77**(1), 13–19 (1981).
44. H. Takiwaki, "Measurement of skin color: practical application and theoretical considerations," *J. Med. Invest.* **44**(3–4), 103–108 (1998).
45. J. A. McGrath and J. Uitto, Chapter 3, "Anatomy and organization of human Skin," *Rook's Textbook of Dermatology*, 7th ed., Vol. 1, pp. 3.2–3.80 Blackwell Publishing, Massachusetts (2004).
46. J. R. Mourant et al., "Mechanisms of light scattering from biological cells relevant to noninvasive optical-tissue diagnostics," *Appl. Opt.* **37**(16), 3586–3593 (1998).
47. I. S. Saidi, S. L. Jacques, and F. K. Tittel, "Mie and Rayleigh modeling of visible-light scattering in neonatal skin," *Appl. Opt.* **34**(31), 7410–7418 (1995).
48. R. Graaff et al., "Reduced light-scattering properties for mixtures of spherical particles: a simple approximation derived from Mie calculations," *Appl. Opt.* **31**(10), 1370–1376 (1992).
49. C. C. Selby, "An electron microscope study of the epidermis of mammalian skin in thin sections. I. Dermo-epidermal junction and basal cell layer," *J. Biophys. Biochem. Cytol.* **1**(5), 429–444 (1955).
50. R. R. Anderson and J. A. Parrish, *The Science of Photomedicine*, Plenum, New York (1982).
51. G. H. Findlay, "Blue skin," *Br. J. Dermatol.* **83**(1), 127–134 (1970).
52. A. Kienle et al., "Why do veins appear blue? A new look at an old question," *Appl. Opt.* **35**(7), 1151–1160 (1996).
53. S. Alaluf et al., "Ethnic variation in melanin content and composition in photoexposed and photoprotected human skin," *Pigment Cell Res.* **15**(2), 112–118 (2002).
54. S. L. Jacques, "Origins of tissue optical properties in the uva, visible, and nir regions," *OSA TOPS on Advances in Optical Imaging and Photon Migration*, R. R. Alfano and J. G. Fujimoto Eds., Vol. 2, pp. 364–371, Optical Society of America (1996).
55. S. A. Prahl, "Light transport in tissue," Ph.D. Thesis, The University of Texas (1998).
56. S. Thomsen, "Anatomic and physiologic factors influencing transcutaneous optical diagnosis of deep-seated lesions," *Proc. SPIE* **3250**, 130–139 (1998).
57. M. Rajadhyaksha et al., "In vivo confocal scanning laser microscopy of human skin: melanin provides strong contrast," *J. Invest. Dermatol.* **104**(6), 946–952 (1995).
58. A. N. Bashkatov et al., "Optical properties of melanin in the skin and skin-like phantoms," *Proc. SPIE* **4162**, 219–226 (2000).
59. E. Salomatina et al., "Optical properties of normal and cancerous human skin in the visible and near-infrared spectral range," *J. Biomed. Opt.* **11**(6), 064026 (2006).
60. A. Bhandari et al., "Modeling optical properties of human skin using Mie theory for particles with different size distributions and refractive indices," *Opt. Express* **19**(15), 14549–14567 (2011).
61. C. Magnain, M. Elias, and J. M. Frigerio, "Skin color modeling using the radiative transfer equation solved by the auxiliary function method: inverse problem," *J. Opt. Soc. Am. A* **25**(7), 1737–1743 (2008).
62. G. Zonios and A. Dimou, "Light scattering spectroscopy of human skin in vivo," *Opt. Express* **17**(3), 1256–1267 (2009).
63. W. Verkrusse et al., "Modelling the effect of wavelength on the pulsed dye-laser treatment of port wine stains," *Appl. Opt.* **32**(4), 393–398 (1993).
64. T. S. Lister, P. A. Wright, and P. H. Chappell, "Light transport through skin," *Lasers Med. Sci.* **26**(6), 719–733 (2011).
65. M. M. Selim et al., "Confocal microscopy study of nerves and blood vessels in untreated and treated port wine stains: preliminary observations," *Dermatol. Surg.* **30**(6), 892–897 (2004).
66. G. Poirier, "Human skin modelling and rendering," M.S. Thesis, University of Waterloo (2003).
67. I. M. Braverman, "The cutaneous microcirculation: ultrastructure and microanatomical organization," *Microcirculation-London* **4**(3), 329–340 (1997).
68. G. V. G. Baranoski, A. Krishnaswamy, and B. Kimmel, "Increasing the predictability of tissue subsurface scattering simulations," *Vis. Comput.* **21**, 265–278 (2005).
69. D. J. Faber et al., "Oxygen saturation-dependent absorption and scattering of blood," *Phys. Rev. Lett.* **93**(2), 028102 (2010).
70. M. Igarashi, "The appearance of human skin," Department of Computer Science in Columbia University, New York (2005).
71. A. N. Bashkatov et al., "Optical properties of human skin, subcutaneous and mucous tissues in the wavelength range from 400 to 2000 nm," *J. Phys. D-Appl. Phys.* **38**(15), 2543–2555 (2005).
72. C. Donner et al., "A layered, heterogeneous reflectance model for acquiring and rendering human skin," *ACM Trans. Graph.* **27** (2008).
73. A. J. Welch and M. J. C. van Gemert, "The Adding-Doubling Method," Chapter 5, pp. 101–117, Plenum Press, New York (1995).
74. W. F. Cheong, S. A. Prahl, and A. J. Welch, "A review of the optical-properties of biological tissues," *IEEE J. Quantum Electron.* **26**(12), 2166–2185 (1990).
75. S. L. Jacques, C. A. Alter, and S. A. Prahl, "Angular dependence of hene laser light scattering by human dermis," *Lasers Life Sci.* **1**, 309–333 (1987).
76. E. K. Chan et al., "Effects of compression on soft tissue optical properties," *IEEE J. Sel. Topics Quantum Electron.* **2**(4), 943–950 (1996).
77. C. R. Simpson et al., "Near-infrared optical properties of ex vivo human skin and subcutaneous tissues measured using the Monte Carlo inversion technique," *Phys. Med. Biol.* **43**(9), 2465–2478 (1998).
78. R. Graaff et al., "Optical properties of human dermis in vitro and in vivo," *Appl. Opt.* **32**(4), 435–447 (1993).
79. G. E. Pierard, "E.M.C.O. guidance for the assessment of skin colour," *Br. J. Dermatol.* **10**(1), 1–11 (2002).
80. L. O. Svaaand et al., "Increase of dermal blood volume fraction reduces the threshold for laser-induced purpura: implications for port wine stain laser treatment," *Lasers Surg. Med.* **34**, 182–188 (2004).
81. G. Zonios and A. Dimou, "Modeling diffuse reflectance from semi-infinite turbid media: application to the study of skin optical properties," *Opt. Express* **14**(19), 8661–8674 (2006).
82. N. Bosschaart et al., "Optical properties of neonatal skin measured in vivo as a function of age and skin pigmentation," *J. Biomed. Opt.* **16**(9), 097003 (2011).
83. A. Torricelli et al., "In vivo optical characterization of human tissues from 610 to 1010 nm by time-resolved reflectance spectroscopy," *Phys. Med. Biol.* **46**(8), 2227–2237 (2001).
84. J. R. Mourant et al., "Predictions and measurements of scattering and absorption over broad wavelength ranges in tissue phantoms," *Appl. Opt.* **36**(4), 949–957 (1997).
85. R. M. P. Doornbos et al., "The determination of in vivo human tissue optical properties and absolute chromophore concentrations using spatially resolved steady-state diffuse reflectance spectroscopy," *Phys. Med. Biol.* **44**(4), 967–981 (1999).
86. J. W. Pickering et al., "Changes in the optical properties (at 632.8 nm) of slowly heated myocardium," *Appl. Opt.* **32**(4), 367–371 (1993).
87. S. Wan, R. R. Anderson, and J. A. Parrish, "Analytical modeling for the optical-properties of the skin with in vitro and in vivo applications," *Photochem. Photobiol.* **34**(4), 493–499 (1981).
88. N. Doegnitz et al., "Determination of the absorption and reduced scattering coefficients of human skin and bladder by spatial frequency domain reflectometry," *Proc. SPIE* **3195**, 102–109 (1998).
89. L. Wang, S. L. Jacques, and L. Zheng, "MCML—Monte Carlo modeling of light transport in multi-layered tissues," *Comput. Methods Program. Biomed.* **47**(2), 131–146 (1995).
90. X. Ma, J. Q. Lu, and X.-H. Hu, "Effect of surface roughness on determination of bulk tissue optical parameters," *Opt. Lett.* **28**(22), 2204–2206 (2003).
91. G. Zonios, J. Bykowski, and N. Kollias, "Skin melanin, hemoglobin, and light scattering properties can be quantitatively assessed in vivo using diffuse reflectance spectroscopy," *J. Invest. Dermatol.* **117**, 1452–1457 (2001).
92. S. A. Prahl, *Optical-Thermal Response of Laser Irradiated Tissue*, Plenum Publishing Corporation, New York (1995).
93. M. J. C. van Gemert et al., "Skin optics," *IEEE Trans. Biomed. Eng.* **36**(12), 1146–1154 (1989).
94. W. A. G. Bruls and J. C. Vanderleun, "Forward scattering properties of human epidermal layers," *Photochem. Photobiol.* **40**(2), 231–242 (1984).
95. L. G. Henyey and J. L. Greenstein, "Diffuse radiation in the galaxy," *Astrophys. J.* **93**, 70–83 (1941).
96. A. Dunn and R. Richards-Kortum, "Three-dimensional computation of light scattering from cells," *IEEE J. Sel. Topics Quantum Electron.* **2**(4), 898–905 (1996).

97. M. Canpolat and J. R. Mourant, "High-angle scattering events strongly affect light collection in clinically relevant measurement geometries for light transport through tissue," *Phys. Med. Biol.* **45**(5), 1127–1140 (2010).
98. D. Toubanc, "Heney-Greenstein and Mie phase functions in Monte Carlo radiative transfer computations," *Appl. Opt.* **35**(18), 3270–3274 (1996).
99. S. K. Sharma, A. K. Roy, and D. J. Somerford, "New approximate phase functions for scattering of unpolarized light by dielectric particles," *J. Quant. Spectrosc. Radiat. Transfer.* **60**(6), 1001–1010 (1998).
100. L. O. Reynolds and N. J. McCormick, "Approximate 2-parameter phase function for light-scattering," *J. Opt. Soc. Am.* **70**(10), 1206–1212 (1980).
101. S. K. Sharma and S. Banerjee, "Role of approximate phase functions in Monte Carlo simulation of light propagation in tissues," *J. Opt. A-Pure Appl. Opt.* **5**(3), 294–302 (2003).
102. Q. Lu and Q. M. Luo, "On phase function of Monte Carlo simulation of light transport in turbid media," *3rd International Conference on Photonics and Imaging in Biology and Medicine*, pp. 122–130, SPIE, Wuhan, China (2003).
103. F. Yongji and S. L. Jacques, "Monte Carlo simulation study on phase function," *Proc. SPIE* **6084**, 608408 (2006).
104. D. H. P. Schneiderheinze, T. R. Hillman, and D. D. Sampson, "Modified discrete particle model of optical scattering in skin tissue accounting for multiparticle scattering," *Opt. Express* **15**(23), 15002–15010 (2007).
105. P. Y. Liu, "A new phase function approximating to mie scattering for radiative transport-equations," *Phys. Med. Biol.* **39**(6), 1025–1036 (1994).
106. H. Ding et al., "Refractive indices of human skin tissues at eight wavelengths and estimated dispersion relations between 300 and 1600 nm," *Phys. Med. Biol.* **51**(6), 1479 (2006).
107. V. V. Tuchin, S. R. Utz, and I. V. Yaroslavsky, "Tissue optics, light-distribution, and spectroscopy," *Opt. Eng.* **33**(10), 3178–3188 (1994).
108. J.-C. Lai et al., "Complex refractive index measurement of biological tissues by attenuated total reflection ellipsometry," *Appl. Opt.* **49**(16), 3235–3238 (2010).
109. G. J. Tearney et al., "Determination of the refractive-index of highly scattering human tissue by optical coherence tomography," *Opt. Lett.* **20**(21), 2258–2260 (1995).
110. A. M. K. Enejder et al., "Influence of cell shape and aggregate formation on the optical properties of flowing whole blood," *Appl. Opt.* **42**(7), 1384–1394 (2003).
111. A. M. K. Nilsson et al., "T-Matrix computations of light scattering by red blood cells," *Appl. Opt.* **37**(13), 2735–2748 (1998).
112. L. G. Lindberg and P. A. Oberg, "Optical-properties of blood in motion," *Opt. Eng.* **32**(2), 253–257 (1993).
113. M. Friebe et al., "Determination of optical properties of human blood in the spectral range 250 to 1100 nm using monte carlo simulations with hematocrit-dependent effective scattering phase function," *J. Biomed. Opt.* **11**(3), 034021 (2006).
114. M. Keijzer et al., "Fluorescence spectroscopy of turbid media—autofluorescence of the human aorta," *Appl. Opt.* **28**(20), 4286–4292 (1989).
115. H. Li, L. Lin, and S. Xie, "Refractive index of human whole blood with different types in the visible and near-infrared ranges," *Proc. SPIE* **3914**, 517–521 (2000).
116. M. Keijzer et al., "Light distributions in artery tissue—monte-carlo simulations for finite-diameter laser-beams," *Lasers Surg. Med.* **9**(2), 148–154 (1989).
117. G. Müller and A. Roggan, *Laser-Induced Interstitial Thermotherapy, Part II, Optical and Thermal Properties of Biological Tissue*, p. 39, SPIE Press, Bellingham, Washington (1995).
118. H. F. Ding et al., "Refractive indices of human skin tissues at eight wavelengths and estimated dispersion relations between 300 and 1600 nm," *Phys. Med. Biol.* **51**(6), 1479–1489 (2006).
119. M. Hammer, A. N. Yaroslavsky, and D. Schweitzer, "A scattering phase function for blood with physiological haematocrit," *Phys. Med. Biol.* **46**(3), N65–N69 (2001).
120. I. Turcu, "Effective phase function for light scattered by blood," *Appl. Opt.* **45**(4), 639–647 (2006).
121. A. N. Yaroslavsky et al., "Different phase function approximations to determine optical properties of blood: a comparison," *Proc. SPIE* **2932**, 324–330 (1997).
122. R. Zhang et al., "Determination of human skin optical properties from spectrophotometric measurements based on optimization by genetic algorithms," *J. Biomed. Opt.* **10**(2), 024030 (2005).
123. O. W. van Assendelft, *Spectrophotometry of Haemoglobin Derivatives*, Royal Vangorcum Ltd. Assen, The Netherlands (1970).